Designing of Fullers-Earth-Containing Poly(vinyl alcohol)-*g*-Poly(2-acrylamido-2-methyl-1-propanesulfonic acid) Nanocomposites: Swelling and Deswelling Behaviors

Rachna Sancha, J. Bajpai, A. K. Bajpai

Bose Memorial Research Laboratory, Government Autonomous Science College, Jabalpur, Madhya Pradesh 482001, India

Received 1 September 2009; accepted 20 February 2010
DOI 10.1002/app.32325
Published online 2 June 2010 in Wiley InterScience (www.interscience.wiley.com).

ABSTRACT: In this study, polymer–clay nanocomposites (PCNs) composed of poly(vinyl alcohol)s (PVAs), poly(2-acrylamido-2-methyl-1-propane sulfonic acid), and fullers earth were prepared by the effective dispersal of inorganic nanoclays in the organic PVA matrix via *in situ* free-radical polymerization with potassium persulfate as an initiator and *N*,*N*-methylene bisacrylamide as a crosslinker. The monomer, 2-acrylamido-2-methyl-1-propane sulfonic acid, was grafted onto the PVA backbone, and at the same time, fullers earth layers were intercalated and exfoliated into the grafted copolymer, especially at a low or moderate loading of the fullers earth. The synthesized PCN materials were characterized by Fourier transform infrared spectroscopy and wide-angle X-ray diffraction techniques. The morphological features of the synthesized materials were studied by scanning electron microscopy; this revealed that the swelling ratio of this nanocomposite increased with increasing fullers earth content. The X-ray diffraction results indicated that the fullers earth was exfoliated in the nanocomposite matrix, and its introduction into the polymer matrix enhanced the percentage crystallinity of the polymer. © 2010 Wiley Periodicals, Inc. J Appl Polym Sci 118: 1230–1239, 2010

Key words: clay; nanocomposites; polyelectrolytes

INTRODUCTION

Polymer–clay nanocomposites (PCNs) are among the most successful nanotechnological materials today. This is because they can simultaneously improve the material properties without significant tradeoffs.[1] In general, nanocomposites exhibit gains in barrier, flame-resistance, structural, and thermal properties without a significant loss in impact or clarity. Because of the nanometer-sized dimensions of the individual platelets in one direction, exfoliated nanoclays are transparent in most polymer systems.[2] Nanocomposites also demonstrate enhanced fire-resistance properties and are finding increasing use in engineering plastics.

These nanocomposites promise new applications in many fields, including mechanically reinforced lightweight components, nonlinear optics, battery cathodes and ionics, nanowires, sensors, and other systems. The general class of organic/inorganic nanocomposites may also be of relevance to issues of bioceramics and biomineralization, in which the *in situ* growth and polymerization of biopolymers and inorganic matrices is occurring.

There are two main methods for obtaining such nanocomposites. One is the direct intercalation of a polymer chain into the host from either the solution or molten state.[4] The other method is the intercalation of a monomer with subsequent chemical thermal *in situ* polymerization.[5] There are lots of applications for polymer clay nanocomposites:[6] increased heat distortion temperature and thermostability, health care, and wound healing; environmental forest and water conservation; fire-extinguishing powders; binding agents for oil on water; animal husbandry; manure treatment; cat litter; water and wastewater purification; sewage sludge palletizing; barriers; and so on.

Fullers earth is a natural earthy material that decolorizes mineral and vegetable oils and has a high sorbent capacity for water and oil. Its applications include carriers for insecticides, pesticides, and fertilizers used in agriculture and absorbers of oil and water spills on the floors of machine shops, factories, service stations, and other manufacturing plants for safety purposes. Montmorillonite (MMT) is the principal clay mineral in fullers earth.[8] The true start of polymer nanocomposite history dates back to 1990 when Toyota first used clay/nylon 6 nanocomposites.[9] Lee and Fu[10] prepared nanocomposites hydrogels from various ratios of *N*-isopropyl

Correspondence to: A. K. Bajpai (akbmrl@yahoo.co.in or akbajpai@yahoo.co.in).

acrylamide and clay MMT. Carrado and Xu[11] prepared polymers containing silicate gels by hydrothermal crystallization to form layered magnesium silicate hectorite clay-containing polymers. Strawhecker and Manias[12] synthesized poly(vinyl alcohol) (PVA)/sodium MMT nanocomposites of various compositions by casting from a polymer/silica water suspension. The composite structure study revealed the coexistence of exfoliated and intercalated fullers earth layers, especially for low and moderate silicate loadings. Bae et al.[13] prepared fully exfoliated nanocomposites by incorporating clay into a polypyrrole graft copolymer. Lim and Park[14] fabricated organic/inorganic hybrid nanocomposites based on poly(styrene–butadiene–styrene) copolymer and clay by melt intercalation. The degree of intercalation was found to be dependent on the surface properties of the clay and poly(styrene–butadiene–styrene) copolymer. It was also shown that the thermal stability of the clay and the surface properties were very important in the fabrication of the polymer/clay nanocomposites.

Botana et al.[15] prepared polymer nanocomposites based on a bacterial biodegradable thermoplastic polyester, polyhydroxybutyrate, and two commercial MMTs, sodium MMT and 30BM (organically modified MMT), by a melt-mixing technique at 165°C. Both clays minerals were characterized by morphology, crystallochemical parameters, and thermal stability. Hwang et al.[16] successfully modified organic clays containing the urethane group by introducing a covalent bond between the silanol group on the clay side and the hydroxyl group of the organic modifier in the silicate layer using 1,6-diisocyanatohexane, namely, surface-treated MMT (30BM), to increase both the basal spacing and the favorable interactions between the clay and the polymer. Marand et al.[17] studied the transport properties of select volatile organic compounds in polyurethane/clay nanocomposite barrier membranes as a function of the clay content. The nanocomposites were fabricated by two different processing methods involving the stirring and sonication of the clay particles.

In this study, we aimed to synthesize PCN components of PVA–poly(2-acrylamido-2-methyl-1-propane sulfonic acid) (PAMPS)[18] and fullers earth and to study their various properties. PVA and PAMPS are well known nonionic and ionic polymers, respectively, and are known for their wide range of biomedical applications.

EXPERIMENTAL

Materials

PVA (molecular weight = 1×10^5 Da, weight-average molecular weight/number-average molecular weight = 2.2, diod syndiotactity = 53%), soluble in hot water, was obtained from Research Chem Industries (Mumbai, India). Fullers earth clay was provided by Loba Chemie (Mumbai, India). 2-Acrylamido-2-methyl-1-propane sulfonic acid (AMPS) was a kind gift from National Chemical Laboratory (Pune, India). Sodium lauryl sulfate, used as a surfactant; *N,N*-methylene bisacrylamide (MBA), used as a crosslinking agent; and potassium persulfate (KPS), used as an initiator, were obtained from Research Loba Chemie (Mumbai, India). Distilled water was used throughout the experiments.

Preparation of the hydrogel

A typical experiment was carried out by the dissolution of 2 g of PVA in 25 mL of distilled water at 60°C with stirring until its complete dissolution. To this solution were sequentially added 1 g of AMPS, 20 mg of MBA, 10 mg of sodium lauryl sulfate, and 20 mg of KPS, and a homogeneous solution was prepared. Polymerization was carried out at 35°C for 1 day. After gelation was completed, the gel membranes were cut into disks 10 mm in diameter and immersed in an excess amount of distilled water for purification. The swollen nanocomposite gels were dried at 25°C for 7 days, and the dried gels were stored in air-tight polythene bags.

Preparation of the nanocomposites

Nanocomposites were prepared by the dispersion of nanoclay into a host polymer, generally at less than 5 wt % levels. This process is known as exfoliation.[19] When nanoclay is substantially dispersed, it is said to be exfoliated. Exfoliation is facilitated by surface compatibilization chemistry, which expands the nanoclay platelets to the point where individual platelets can be separated from one another by mechanical shear or heat of polymerization.[20]

For the preparation of the fullers earth–polymer nanocomposites, 2 g of PVA was dissolved in 25 mL of distilled water at 60°C, and 1 g of AMPS was added to it. After complete dissolution, definite amounts of surfactant and the MBA corresponding agent, fullers earth, were added, and crosslinking polymerization was carried out as described previously.

Characterization

Fourier transform infrared (FTIR) spectroscopy

To ascertain the types of interaction present between the polymer and the clay, the FTIR spectra of the native fullers earth and PVA, AMPS-grafted PVA, and fullers earth were recorded on a PerkinElmer spectrophotometer.

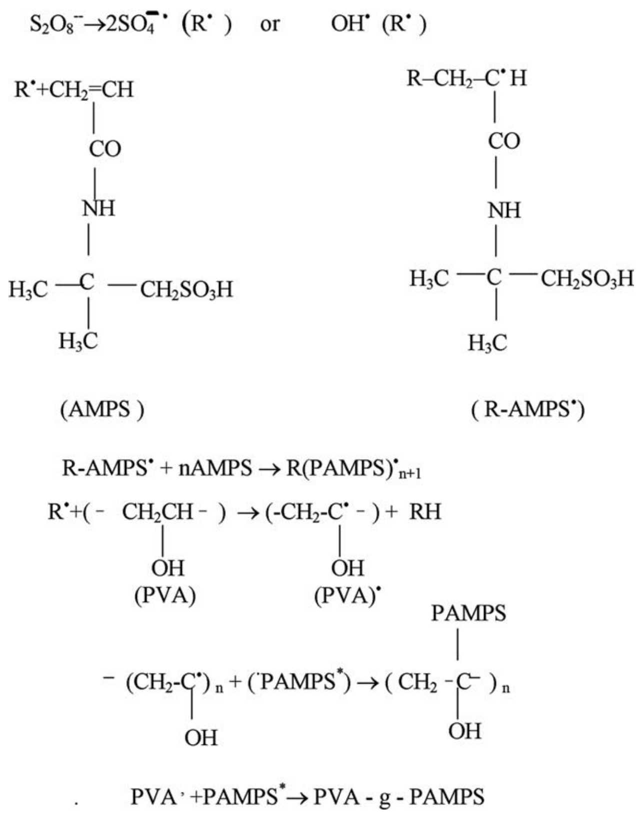

Figure 1 Mechanism of the grafting of AMPS onto the PVA backbone.

X-ray diffraction (XRD)

The fullers earth and nanocomposites were characterized by the X-ray powder diffraction method. For the analysis of the basal spacing of the clay, the fullers earth powder was mounted on a sample holder with a large cavity, and we obtained a smooth surface by pressing the powder with a glass plate. We analyzed the gels by spreading the mixture on a gel membrane used as a sample holder. Powder XRD analysis was performed with a Siemens D5000 diffractometer (Berlin, Germany) with Cu radiation (40 kV, 30 mA). The speed was 3°/min.

Scanning electron microscopy (SEM)

The morphologies were examined with SEM (StereoScan430, Leica) USA with an acceleration voltage of 20 kV.

Swelling studies

The dry gels were immersed in an excess amount of deionized water at room temperature until the swelling equilibrium was attained. The weight of the swollen sample was determined after removal of the surface water by gentle blotting with filter paper. The dry weight was recorded after the gel was dried in an oven for 1 day. The swelling ratio was calculated with the following equation:

$$\text{Equilibrium swelling ratio} = \frac{(W_s - W_d)}{W_d}$$

where W_s and W_d are the weights of the swollen and dry gels, respectively.

Shrinking ratio

The shrinking or deswelling of the gel was performed by the adoption of a gravimetric procedure. In this procedure, a fully swollen gel was allowed to dry at a definite temperature (25°C), and the drying gel was weighed at different time intervals to determine its swelling ratio at respective time periods.

The shrinking ratio was calculated with the following equation:

$$\text{Shrinking ratio } (\%) = \frac{(SR_e - SR_t)}{SR_e} \times 100$$

where SR_e and SR_t are the initial equilibrium swelling ratio and the swelling ratio of the gel at shrinking time t, respectively.

Statistical analysis

All experiments were done at least three times, and the swelling results, expressed as curves, are shown along with error bars. The data obtained were found to show a fair level of reproducibility and are represented as the mean plus or minus the standard deviation.

RESULTS AND DISCUSSION

Preparative reaction schemes

A typical synthesis of clay–polymer nanocomposites involves the dispersion of clay into a reaction mixture containing monomer and polymer and subsequent polymerization. The synthesis of the hydrogel and fullers earth–polymer nanocomposite are schematically shown in Figures 1 and 2, respectively. It is clear from the reaction scheme that the persulfate and/or hydroxyl radicals (R·) attacked the PVA and monomer (AMPS) to yield radicals of PVA and AMPS, respectively. The AMPS radicals attack the new monomer molecules and formed macroradicals (PAMPS·), which further added to the PVA radicals to produce a grafted polymer.

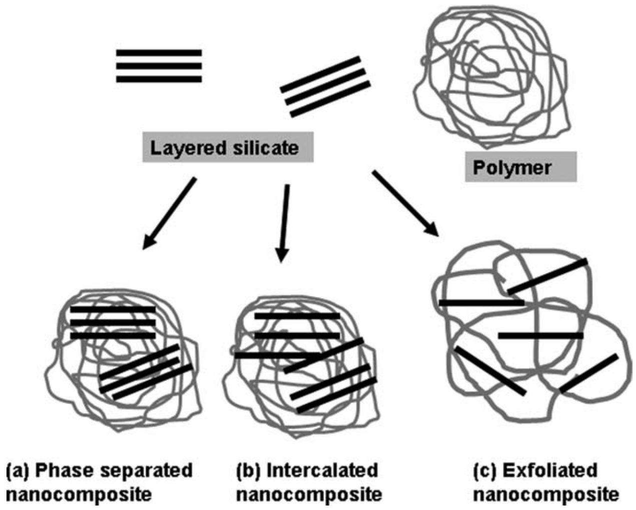

Figure 2 Scheme of the formation of the PCNs.

Physical appearance

Figure 3(a,b) show the photographs of native gel and gel with exfoliated fullers earth composite; these provide clear evidence for the formation of the clay–polymer nanocomposite. As evident from the photograph, although the native gel was transparent in color, the clay-intercalated gel appeared light yellow; this may have been due to the formation of interpenetrating networks or clay nanocomposites.

FTIR spectra

FTIR spectral analysis has been widely used to characterize PCNs. The FTIR spectra of fullers earth, native grafted polymer, and clay–polymer nanocomposite are shown in Figure 4(a,b), respectively. The

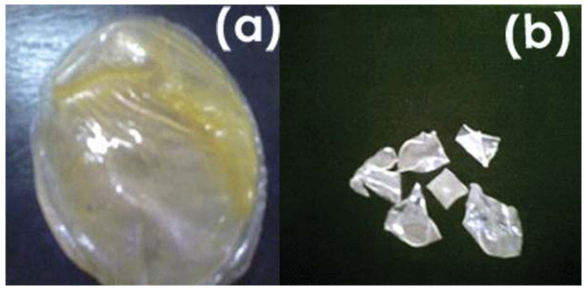

Figure 3 Physical appearance of the gels: (a) native gel and (b) gel with fullers earth composite. [Color figure can be viewed in the online issue, which is available at www.interscience.wiley.com.]

spectra of fullers earth clearly indicated the abundance of clay hydroxides, as evident from the observed broad bands at 3628 cm^{-1}. Characteristic bands, including OH stretching at 3672 cm^{-1} and —Si—O stretching at 929 cm^{-1}, were due to the humid substances present in the soil, which contained organic compounds. Some of these compounds contained carbonyl groups, so it was expected that the IR spectrum should depict the characteristic peaks of C=O at 1676 cm^{-1}, strong C=O asymmetrical stretching at 3089 cm^{-1}, and weak C=O symmetrical stretching at 1676 cm^{-1}. The grafted copolymer showed broad absorption bands at 3147 cm^{-1} due to the OH groups of PVA, and the additional bands observed at 1157, 1676, and 1608 cm^{-1} could have been assignable to SO_3H, CO, and CONH groups (stretching mode), respectively. Hence, the presence of such additional bands in the graft copolymer indicated the occurrence of grafting.[21–24] The mechanism of grafting of PAMPS chains onto PVA in the presence of KPS as a free-radical initiator is suggested, as

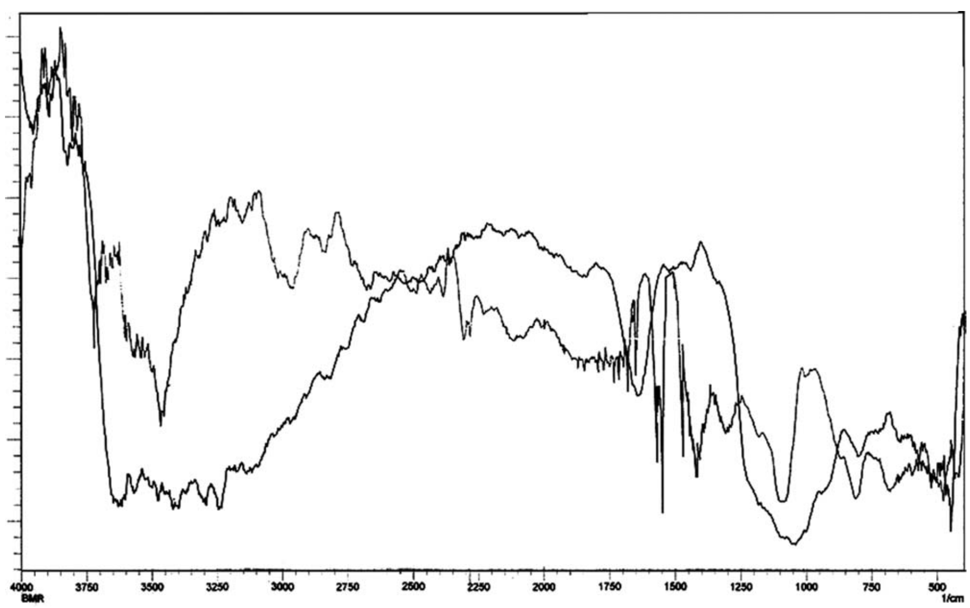

Figure 4 FTIR spectra of the native fuller earth (b) PCN.

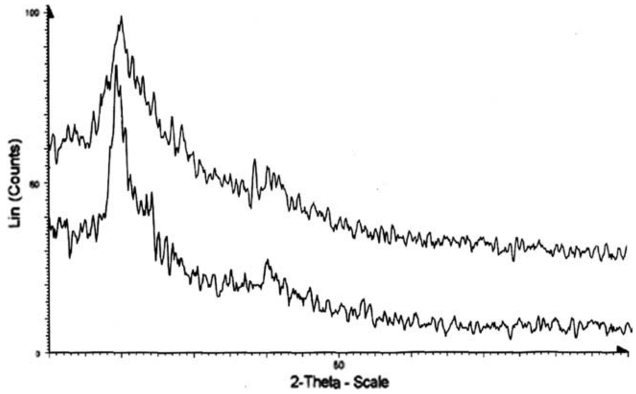

Figure 5 XRD patterns of the (a) native grafted polymer and (b) PCN.

shown in Figure 1.[25] The existence of PVA and fullers earth in the fully extracted nanocomposites suggested the exfoliation of a fullers earth layer within the polymer matrix.

XRD analysis

XRD measurements are quite useful in the determination of the basal spacing (d_{100}) of the crystalline phase in the nanocomposite. In this study, the XRD spectra of the grafted polymer and nanocomposites were recorded, as shown in Figure 5(a,b), respectively. The XRD spectra showed a strong peak near a 2θ value of 20°, which corresponded to the plane (100) of the PVA, whereas other minor peaks around 22–24° were attributed to the low crystallinity of the matrix due to grafted PAMPS chains. The polymer matrix had greater crystallinity, as evident from the increase in the sharpness of the peaks in the XRD spectra, as shown in Figure 5(b).The increase in crystallinity was due to the formation of the clay–polymer. nanocomposites.[26,27]

The physical and mechanical properties of a polymer are profoundly dependent on the degree of crystallinity. The percentage crystallinity was calculated for the fullers earth nanocomposites. The numerical formula to calculate the percentage crystallinity is given in the following equation:

$$\text{Crystallinity}\,(\%) = \frac{A_C}{A_a + A_C}$$

where A_C and A_a are the areas of the crystalline and amorphous phases, respectively. The percentage crystallinity of the fullers earth nanocomposite was calculated to be 17.17%, and without fullers earth, it was 14.37%. Scientifically, PVA is known to be semicrystalline in nature; the increase in crystallinity was due to the formation of clay–polymer nanocomposites.

SEM

The morphological features of the prepared grafted matrix and clay nanocomposite were studied through the SEM images of the native gel and nanocomposite, as shown in Figure 6(a,b), respectively. It is clear from Figure 6(a) that the surface of the native grafted gel was a little bit heterogeneous and uneven. After the addition of clay to the polymer redox reaction mixture and upon subsequent polymerization, the nanocomposite formed depicted a much more heterogeneous morphology, as shown in Figure 6(b). The observed heterogeneity may have been due to the aggregation of fullers earth nanocomposites due to the increased viscosity of the polymerization medium. After the addition of clay to the polymerization reaction mixture and upon subsequent polymerization, the nanocomposite formed depicted a much more heterogeneous morphology, as shown in Figure 6(b). It is clear from the image that the aggregated particles varied in size from 5 to 20 μm.

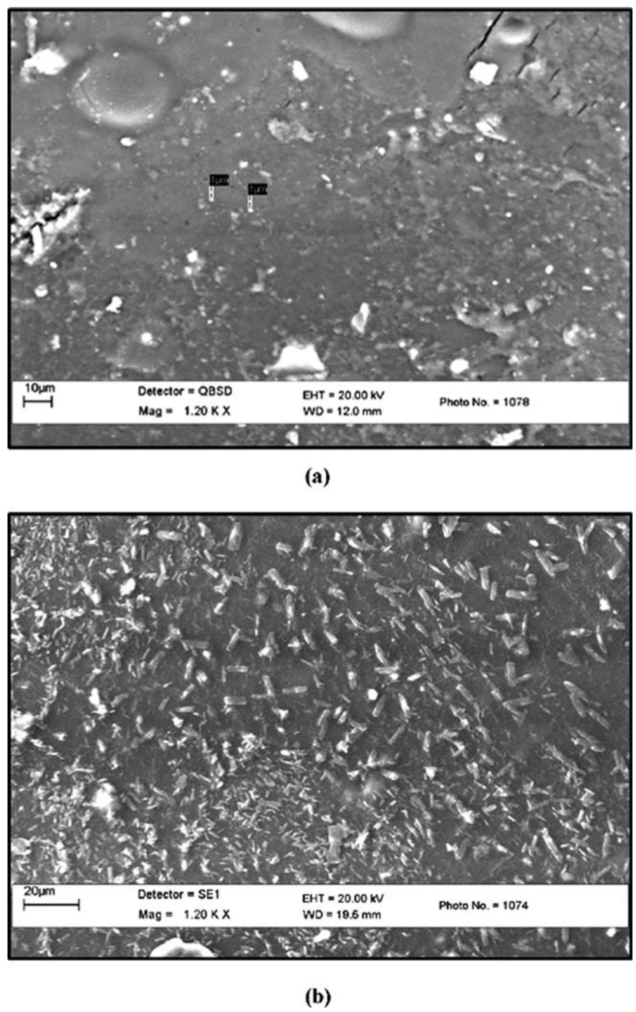

Figure 6 SEM images of the (a) unloaded and (b) loaded fullers earth polymers.

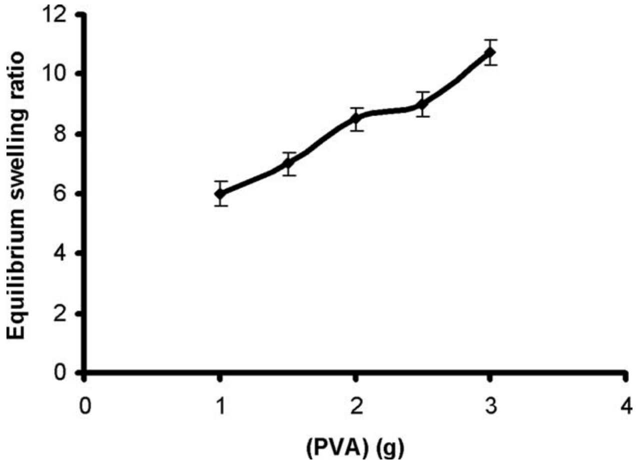

Figure 7 Effect of PVA on the swelling ratio of the nanocomposite.

Swelling results and effect of the ingredients

The swelling kinetics of the clay nanocomposites with different weight ratios of ingredients were studied, and we found that the swelling of the gel varied with the composition of the nanocomposite matrix, as discussed later.

Effect of PVA

To study the effect of PVA on the swelling ratio, we varied the amount of PVA in the range 1.0–3.0 g and kept the quantities of the other ingredients constant. The results shown in Figure 7 reveal that when the amount of PVA in the gel increased up to 3.0 g, the swelling ratio of the gel also increased. The results may be explained by fact that with increasing amount of PVA, the hydrophilicity of the matrix increased, which brought about an increase in the swelling ratio. Moreover, the increased amount of PVA also resulted in increases in the mesh sizes of the network, which also resulted in an enhanced swelling.[28,29]

Effect of the monomer (AMPS)

To study the influence of AMPS variation on the swelling ratio of the nanocomposites, we varied the concentration of AMPS in the range 2.4–12.2 m*M* and kept the other constituent concentrations constant. The results are shown in Figure 8, which indicates that the equilibrium swelling ratio increased with increasing concentration of AMPS in the range 2.4–7.12 m*M*, whereas beyond 7.12 m*M*, a fall was observed. The observed increases in swelling may have been due to the fact that with increasing AMPS concentration, the number of charged centers present along the polymer chains increased, which due to mutual repulsion, caused the rapid relaxation of polymer chains. This clearly resulted in a greater amount of water sorption. However, beyond a definite concentration of AMPS, that is, 7.12 m*M*, the swelling ratio fell. The observed decrease in the swelling ratio may have been due to the fact that at a much greater concentration of monomer (AMPS), the formation of homopolymer (PAMPS) may have increased the viscosity of the reaction medium, which translated into a reduced relaxation of the PAMPS chains. This clearly resulted in lower water sorption.

Effect of the initiator (KPS)

The effect of the initiator (KPS) on the swelling of the gel was investigated in the range 9.21×10^{-2} to 73.9×10^{-2} m*M*. The results are shown in Figure 9, which indicates that the swelling of the nanocomposite increased with increasing concentration range of KPS from 9.2×10^{-2} to 18.4×10^{-2} m*M*; beyond a 18.4×10^{-2} m*M* concentration of initiator, the swelling of the gel decreased. The observed results could be explained on the basis of the fact that because the average molecular weight of the grafted copolymer formed was inversely proportional to the imitator concentration, at a lower concentration of persulfate, longer chains of the copolymers of AMPS and PVA were formed, which produced larger free volumes between the polymeric chains in the gel. However, at higher concentrations of persulfate, the average molecular weight of the copolymer was lower, and this, consequently, produces a network of the smaller free volumes, which in turn resulted in a lower degree of water sorption.

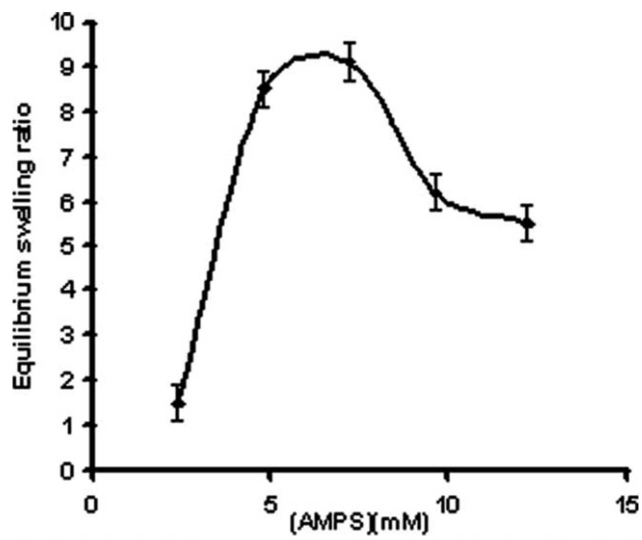

Figure 8 Effect of AMPS on the swelling ratio of the nanocomposite.

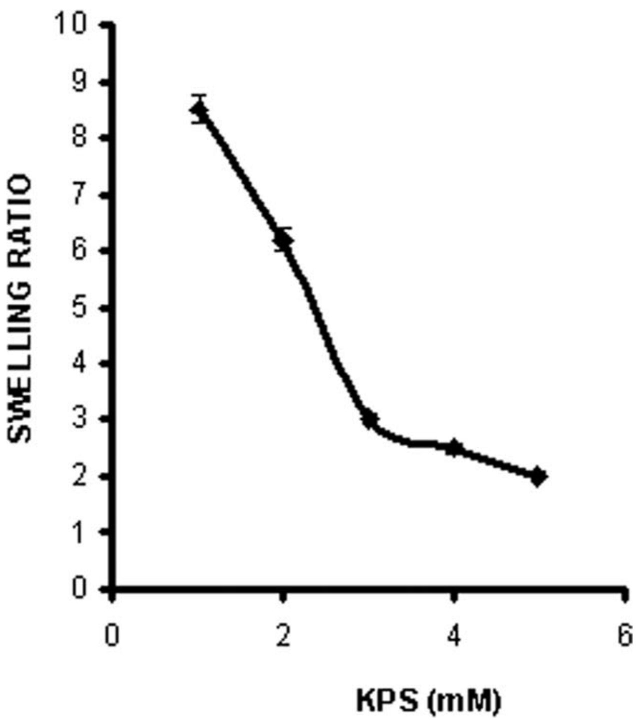

Figure 9 Effect of KPS on the swelling ratio of the nanocomposite.

Effect of the crosslinker (MBA)

We studied the effect of MBA on the swelling of gel by varying its concentration in the range 12.9×10^{-2} to 129.7×10^{-2} m*M* and keeping the other concentration curves constant. The results are shown in Figure 10, which indicates that with an initial increase in the concentration of MBA, the swelling of the gel increased. This was due to the hydrophilic nature of the crosslinker, which tended to imbibe a greater amount of water. However, the relatively higher concentration of crosslinker could have caused a decrease in the swelling ratio of the gel. The reason was quite obvious, as with an increase in the degree of crosslinking, the free volume of the hydrogel network decreased, and thus, a lower number of water molecules entered the gel.

Effect of the clay (fullers earth)

We studied the effect of fullers earth on the swelling of the gel by varying the amount of the fullers earth in the range 20–200 mg. The results are shown in Figure 11, which indicate that with increasing amount of fullers earth in the range 20–100 mg, the swelling of the gel increased because the clay was fully exfoliated in the gel matrix. Although with further increases in the amount of fullers earth, the swelling ratio of the gel decreased; this may have been due to the agglomeration of fullers earth at a high concentration of the clay.

Effect of the temperature

We studied the effect of the temperature on the swelling ratio of the nanocomposite by varying the temperature of the swelling bath in the range 5–70°C. The results are shown in Figure 12, which clearly reveals that the swelling ratio constantly increased with increasing temperature in the studied range. The observed increase in the swelling ratio with increasing temperature may be explained by the fact that a rise in the temperature resulted in increases in both the rate of the diffusion of water molecules and the segmental mobility of the nanocomposite chains, which together resulted in higher swelling.

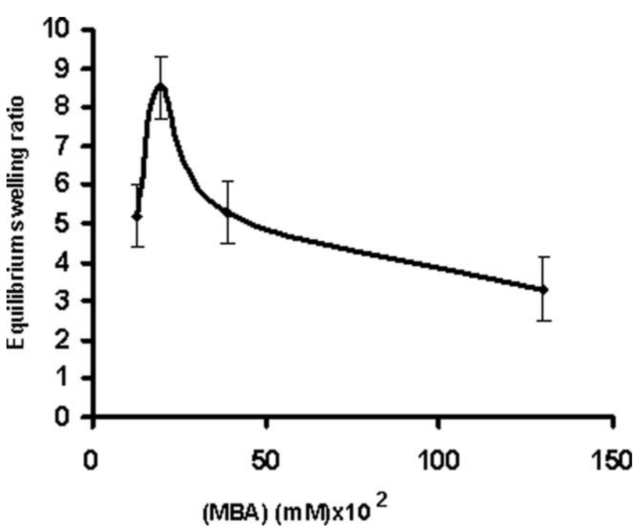

Figure 10 Effect of MBA on the swelling ratio of the nanocomposite.

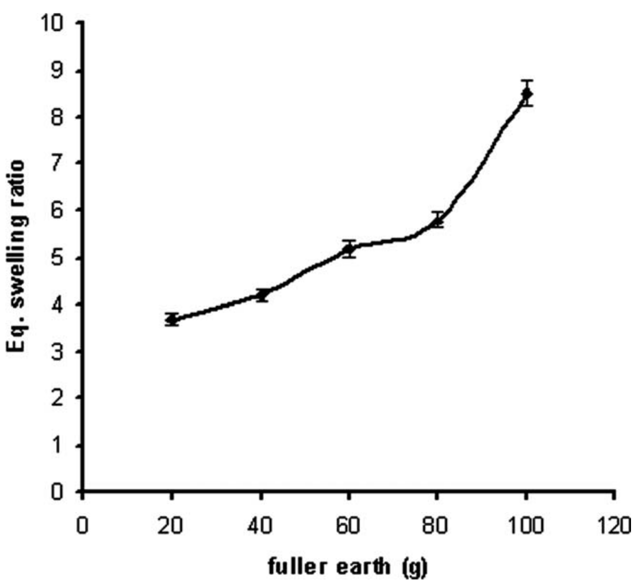

Figure 11 Effect of fullers earth on the swelling ratio of the nanocomposite.

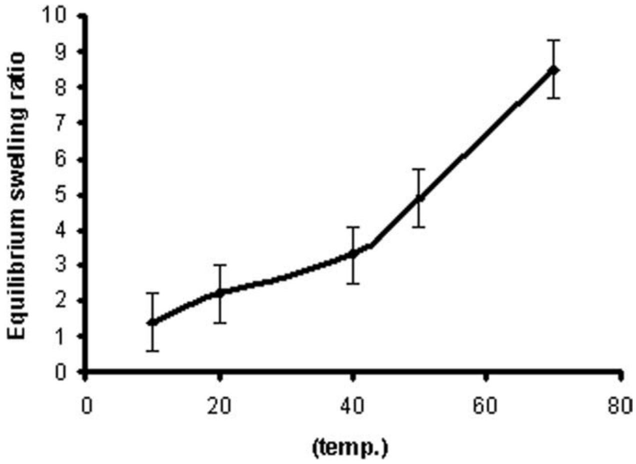

Figure 12 Effect of the temperature on the swelling ratio of the nanocomposite.

Effect of the pH

We investigated the influence of pH on the water-intake capacity of the nanocomposite by adjusting pH of the swelling medium in the range 1.6–12.5. The results are shown in Figure 13, which indicates that initially, the swelling ratio decreased with increasing pH up to 7.0 and, thereafter, increased with increasing pH. The results were attributed to the fact in the initial pH range of suspension, the silanols and aluminols were protonated and, with increasing pH, their positive charges kept decreasing because of the following equations:[30]

$$SiOH_2^+ \xrightarrow{-H^+} SiOH$$

$$AlOH_2^+ \xrightarrow{-H^+} AlOH$$

Thus, because of neutral nature of silanol and aluminols groups, the interaction between there groups and PVA was less favored, and the swelling of the gel decreased. However, at alkaline pH (12.5), the silanols and aluminols ionized, as shown in the following equations:

$$SiOH \xrightarrow{-H^+} SiO^-$$

$$AlOH \xrightarrow{-H^+} AlO^-$$

Thus, the polymer molecules interacted strongly with these charged centers, and as a consequence, the swelling of the gel increased.

Shrinking results and the effect of the ingredients

The shrinking of the gel was evaluated by a gravimetric method that involved weighing the swollen gel and drying it until shrinking equilibrium was attained. The clay nanocomposite gel was immersed in an excess amount of water and then placed at room temperature until equilibrium shrinking was achieved. From the linear portion of the shrinking ratio versus time plot, the shrinking rate was calculated. The influence of the chemical composition on the shrinking rate of the drying nanocomposites are discussed in the following text.

Effect of PVA

We investigated the effect of the PVA content in the nanocomposite on its shrinking behavior by varying the amount of PVA in the range 1.0–3.0 g and monitoring the shrinking ratio of the respective gels. For this purpose, the clay nanocomposite gel was immersed in an excess amount of water and then placed at room temperature until shrinking was achieved. The results are summarized in Table I, which shows that the shrinking ratio constantly decreased with increasing amount of PVA. The results may have been due to the fact that with increasing PVA, the volume fraction of the polymer increased in the gel; this resulted in a gel matrix with smaller mesh sizes and enhanced compactness. The reduction in the mesh sizes of the network resulted in a lower rate of water evaporation as the shrunk mesh of the hydrogel network allowed a lower number of water molecules to pass through the polymer, and the gel evaporated. Furthermore, because the PVA is hydrophilic in nature its increasing amount in the nanocomposite make the matrix more hydrophilic and, therefore, the shrinking rate decreases.

Effect of the monomer (AMPS)

We studied the influence of PAMPS on the shrinking rate of the nanocomposite by increasing the

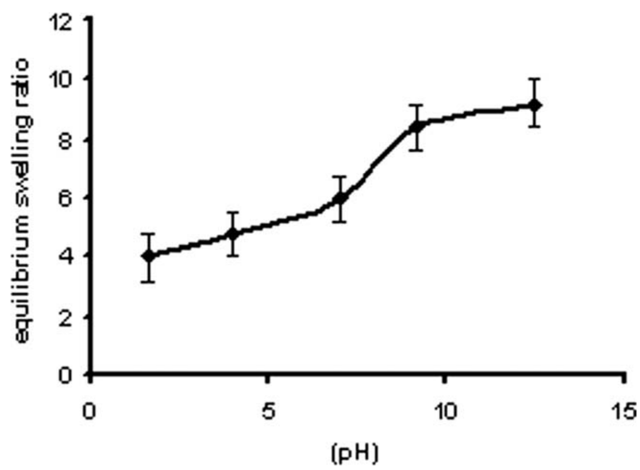

Figure 13 Effect of pH on the swelling ratio of the nanocomposite.

TABLE I
Data Showing the Effect of the Composition of the Nanocomposite on the Shrinking Rate and Equilibrium Swelling Ratio

PVA content (g)	Other ingredients	Shrinking rate per minute
1.0	AMPS, 4.8 m*M*	6.0 ± 0.16%
1.5	Fullers earth, 100 mg	5.0 ± 0.15%
2.0	KPS, 9.2×10^{-2} m*M*	2.0 ± 0.08%
2.5	MBA, 19.45×10^{-2} m*M*	3.0 ± 0.09%
3.0		5.0 ± 0.16%
AMPS content (m*M*)	**Other ingredients**	**Shrinking rate per minute**
2.4	PVA, 2 g	2.0 ± 0.09%
4.8	Fullers earth, 100 mg	5.0 ± 0.14%
7.21	KPS, 9.2×10^{-2} m*M*	6.0 ± 0.19%
9.61	MBA, 19.45×10^{-2} m*M*	7.2 ± 0.20%
12.2		8.5 ± 0.30%
Fullers earth (mg)	**Other ingredients**	**Shrinking rate per minute**
20	PVA, 2 g	6.0 ± 0.20%
40	AMPS, 4.8 m*M*	5.4 ± 0.19%
60	KPS, 9.2×10^{-2} m*M*	5.0 ± 0.15%
80	MBA, 19.45×10^{-2} m*M*	4.0 ± 0.13%
100		2.0 ± 0.07%

concentration of AMPS in the feed mixture in the range 2.4–12.2 m*M*. The results are presented in Table I, which reveals that the shrinking rate increased with increasing PAMPS content. The results may have been due to the fact that increasing the proportion of the ionic component (PAMPS) in the composite resulted in an increased relaxation of the polymer chain due to repulsion between the anionic groups present along the PAMPS chains. Because of the increased relaxation, the mesh sizes of the network widened and resulted in a greater water evaporation rate. This clearly brought about an increase in the shrinking rate of the nanocomposite.

Effect of the clay (fullers earth)

The presence of fullers earth markedly influenced not only the mechanical and thermal properties[31] but also the shrinking rate of the nanocomposite, as the added clay was expected to block the pores of the network and may have resulted in a decrease in the shrinking rate. In this study, we investigated the effect of fullers earth on the shrinking rate of the nanocomposite by varying the amount of fullers earth in the range 20–200 mg. The results summarized in Table I indicate that the shrinking rate decreased with increasing amount of fullers earth in the nanocomposite. The observed decrease may have been due to the fact that the added fullers earth accumulated at the openings of the meshes of the network and reduced the mesh size. This reduction in mesh sizes obviously resulted in a decreased rate of water evaporation and led to a decreased shrinking rate.

CONCLUSIONS

The redox polymerization of AMPS in the immediate presence of PVA and fullers earth resulted in a clay–polymer nanocomposite, as evident from the structural characterization as confirmed by FTIR analysis.

The XRD spectra of the clay–polymer nanocomposite indicated an increase in the crystallinity of the polymer matrix due to the intercalation and exfoliation of the fullers earth. The nanocomposite showed a heterogeneous morphology with aggregated particles varying in the range 5–20 μm.

When the amount of PVA was increased in the range 1.0–3.0 g, the nanocomposite showed a greater water sorption capacity. In the case of AMPS, the swelling ratio initially increased with increasing AMPS from 2.4 to 7.12 m*M*; at a higher concentration of AMPS (beyond 7.12 m*M*), a decrease in the swelling ratio was observed. The swelling ratio also increased in the range 9.2–18.4 $\times$ 10^{-2} m*M* of KPS, whereas beyond 18.4 $\times$ 10^{-2} m*M*, the water sorption capacity of the nanocomposite decreased. In the case of a variation in the concentration of the crosslinking agent (MBA), we observed that initially, with increasing concentration of MBA, the swelling ratio increased, whereas at a higher MBA concentration, a decrease in the swelling ratio was noticed. The swelling behavior of the nanocomposite also depended on the composition of the matrix. The amount of fullers earth, when varied from 20 to 100 mg, resulted in an increased swelling of the nanocomposite, whereas beyond 100 mg, a fall in the swelling ratio was observed. When the temperature and pH of the outer swelling medium increased, the swelling ratio constantly increased.

The shrinking behavior of the nanocomposite also depended on the chemical composition of the nanocomposite. With increasing the amount of PVA and fullers earth, the shrinking rate deceased, whereas with increasing AMPS, the shrinking rate increased.

References

1. Heller, H.; Mehmud, C. H.; Tombull, W. H. The University Text of Nanotechnology; Dominant: New Delhi, India, 2000; Vol. 2, p 127.
2. Chung, T. C.; Manias, E.; Wang, Z. M. U.S. Pat. 7,829 (2007).
3. Dobsis, A. M. Mater Sci Eng 2000, 28, 63.
4. Okamoto, M. Polymer/Clay Nanocomposites; American Scientific: Stevenson Ranch, CA, 2004; Vol. 8, p 2.
5. Zeng, Q. H.; Wang, D. Z.; Yu, A. B.; Lu, G. Q. The Nonmaterial Centre of Engineering, University of Queensland, Australia, 2000, 13, 549.
6. Giannelis, E. P. Appl Organomet Chem 1998, 12, 675.
7. Roskill Information Services. The Economics of Bentonite, Fuller's Earth, and Allied Clays, 7th ed.; Roskill Information Services: London, 1994; Vol. 7, p 91.
8. Biswas, M.; Sinha, R. S. Adv Polym Sci 2001, 155, 221.
9. Cho, J. W.; Paul, D. R. Polymer 2001, 42, 1094.
10. Lee, F. W.; Fu, Y. T. J Appl Polym Sci 2003, 89, 3652.
11. Carrado, K. A.; Xu, L. Chem Mater 1998, 10, 1445.
12. Strawhecker, K. E.; Manias, E. Chem Mater 2000, 2943, 1213.
13. Bae, W. J.; Kim, K. H.; Jo, W. H.; Park, Y. H. Macromolecules 2004, 37, 9854.
14. Yong, T. L.; Park, O. O. J Chem Eng 2001, 18, 25.
15. Botana, A.; Mollo, M.; Eisenberg, P.; Torres Sanchez, R. M. Appl Clay Sci, to appear.
16. Hwang, S. Y.; Yoo, E. S.; Im, S. S. Polymer Degrad Stab 2009, 94, 2163.
17. Herrera-Alonso, J. M.; Marand, E.; Little, J.; Cox, S. S. Eng Fract Mech 2009, 76, 2846.
18. Yassin, A. Polym Int 2001, 50, 353.
19. Hirokawa, Y.; Tanaka, T. J. Chem Phys 1984, 81, 6379.
20. Kato, M.; Usuki, A.; Okada, A. J Appl Polym Sci 1997, 661, 1785.
21. Wu, J.; Lerner, M. M. Chem Mate 993, 5, 836.
22. Hoffman, S. J Controlled Release 1987, 6, 297.
23. Ricka, J.; Tanaka, T. Macromolecules 1984, 17, 2916.
24. Mishra, S.; Panda, A.; Sing, B. J Phys Chem 1997, 63, 679.
25. Gacitua, W. E., Bathlini, A. A., Zhang, J. Rev Ciccia Technol 2005, 7, 154.
26. Greenland, D. J. J Colloid Sci 1963, 18, 64.
27. Bajpai, A. K.; Vishwakerma, N. J. Colloid Interface Sci A 2000, 39, 1248.
28. Giannelis, E. P. Adv Mater 1996, 8, 29.
29. Bajpai, A. K.; Mishra, S. J Mater Sci Mater Med 2006, 17, 1313.
30. Bajpai, A. K.; Vishwakerma, N. J Appl Polym Sci 1994, 51, 651.
31. LeBaron, P. C.; Wang, Z.; Pinnavaia, T. J. Appl Clay Sci 1999, 15, 11.